



# The effect of inhibiting hindbrain A2 noradrenergic neurons by 6-Hydroxydopamine on lipopolysaccharide-treated male rats autistic animal model

Hussain N. Alhamami<sup>a,\*</sup>, Abdullah M. Albogami<sup>a</sup>, Mohammad M. Algahtani<sup>a</sup>,  
Mohammed Alqinyah<sup>a</sup>, Wael A. Alanazi<sup>a</sup>, Fawaz Alasmari<sup>a</sup>, Khalid Alhazzani<sup>a</sup>,  
Ahmed Z. Alanazi<sup>a</sup>, Yasseen A. Alasmrri<sup>a</sup>, Abdullah S. Alhamed<sup>a,\*</sup>

<sup>a</sup> Department of Pharmacology and Toxicology, College of Pharmacy, King Saud University, Riyadh 11451, Saudi Arabia

## ARTICLE INFO

### Keywords:

6-hydroxydopamine  
A2 neurons  
Neuroinflammation  
Prefrontal cortex  
Hippocampus  
Autism spectrum disorder

## ABSTRACT

Autism spectrum disorder (ASD) is a complex neurodevelopmental illness that often emerges in early childhood. The incidence of ASD has shown a notable rise in recent years. ASD is defined by deficits in social communication, and presence of rigid and repetitive behaviors and interests. The underlying mechanisms of ASD remain elusive. Multiple studies have documented the presence of neuroinflammation and increased levels of inflammatory cytokines, specifically, IL-6, TNF, and NF- $\kappa$ B, in various brain regions, including the prefrontal cortex (PFC) and hippocampus in individuals with ASD. Noradrenergic neurons play a crucial role in brain development and the regulation of motor, behavioral, and memory functions. This study sought to examine the impact of intracerebroventricular (icv.) injection of the neurotoxin, 6-hydroxydopamine (6-OHDA), in the caudal dorsal vagal complex A2 neurons on various neuroinflammatory pathways at the hippocampus and PFC in valproic acid (VPA) autistic animal model. This was done in conjunction with an intraperitoneal (i.p.) injection of Lipopolysaccharides (LPS) in animal models with VPA-induced autism. We specifically examined the impact of the caudal fourth ventricle 6-OHDA icv. injection and LPS (i.p.) injection on self-grooming behavior. We measured the mRNA expression of IL-6, TNF- $\alpha$ , and NF- $\kappa$ B using qRT-PCR, and the protein expression of COX-2, GPX-1, p-AMPK, and AMPK using western blot analysis. The self-grooming activity was considerably higher in the combined treatment group (6-OHDA icv. + LPS i.p.) compared to the control group. A substantial increase observed in the expression of IL-6, TNF- $\alpha$ , and NF- $\kappa$ B genes in the PFC of the treatment group that received icv. Administration of 6-OHDA, compared to the control group. The VPA-autism rats that received the combo treatment exhibited a slight increase in the expression level of NF- $\kappa$ B gene in the hippocampus, compared to the control group. At the PFC, we noticed a substantial drop in the expression of the antioxidant protein GPX-1 in the group that received the combo treatment compared to the control group. Our data investigates a novel aspect that the 6-OHDA-induced inhibition of hindbrain A2 neurons could be influencing the neuroinflammatory pathways in the PFC and hippocampus of autistic animal models.

## 1. Introduction

ASD is a prevalent neurodevelopmental disorder often diagnosed during the first three years of childhood. Leo Kanner, a psychiatrist, provided the initial description of ASD in 1943 (Lord et al., 2020). The worldwide incidence rate of ASD is around 1 in 100 children (Zeidan et al., 2022). By 2025, the expenses associated with the treatment and management of ASD in the United States are projected to surpass the

costs of caring for other conditions, including attention deficit hyperactivity disorder (ADHD) and diabetes, both in terms of medical and non-medical expenditures (Wong, 2022). ASD is classified as a multifactorial disorder that arises from the interplay between genetic and environmental variables (Park et al., 2016). ASD can be influenced by environmental factors such as exposure to teratogens like valproic acid and thalidomide during pregnancy, as well as other factors like the short time between pregnancies, multiple pregnancies, maternal obesity,

\* Corresponding authors.

E-mail addresses: [halhamami@ksu.edu.sa](mailto:halhamami@ksu.edu.sa) (H.N. Alhamami), [439106079@student.ksu.edu.sa](mailto:439106079@student.ksu.edu.sa) (A.M. Albogami), [mohgahtani@ksu.edu.sa](mailto:mohgahtani@ksu.edu.sa) (M.M. Algahtani), [malqinyah@ksu.edu.sa](mailto:malqinyah@ksu.edu.sa) (M. Alqinyah), [waanazi@ksu.edu.sa](mailto:waanazi@ksu.edu.sa) (W.A. Alanazi), [ffalasmari@ksu.edu.sa](mailto:ffalasmari@ksu.edu.sa) (F. Alasmari), [kalhazzani@ksu.edu.sa](mailto:kalhazzani@ksu.edu.sa) (K. Alhazzani), [azalanazi@ksu.edu.sa](mailto:azalanazi@ksu.edu.sa) (A.Z. Alanazi), [442105385@student.ksu.edu.sa](mailto:442105385@student.ksu.edu.sa) (Y.A. Alasmrri), [asalhamed@ksu.edu.sa](mailto:asalhamed@ksu.edu.sa) (A.S. Alhamed).

<https://doi.org/10.1016/j.jsps.2024.101964>

Received 10 December 2023; Accepted 21 January 2024

Available online 23 January 2024

1319-0164/© 2024 The Author(s). Published by Elsevier B.V. on behalf of King Saud University. This is an open access article under the CC BY-NC-ND license (<http://creativecommons.org/licenses/by-nc-nd/4.0/>).

gestational bleeding, gestational diabetes, advanced parental age, and infections (Hyman et al., 2020). The Diagnostic and Statistical Manual of Mental Disorders, Fifth Edition (DSM-V), is the current global standard for diagnosing patients with ASD. The DSM-V is comprised of two primary domains: deficiencies in social communication and social interaction and restricting and repetitive patterns of behavior.

ASD is characterized by many neuroanatomical abnormalities, such as particular changes in the size of specific brain regions, altered long-range connections between distinct brain areas, modifications in grey or white matter, and precise microstructural or cellular changes (Donovan & Basson, 2017). The prefrontal cortex (PFC) is a region of the human brain that is part of the cerebral cortex. It is situated in the frontal lobe, positioned in front of the primary motor cortex and the premotor cortex. The PFC is composed of the lateral, medial, and orbital regions, specifically the orbitofrontal cortex (Akkoc RF, Ogeturk M. 2016). The PFC plays a crucial role in regulating several cognitive processes in the brain, such as decision-making, planning, working memory, emotions, social behaviors, learning, and communication. The primary documented changes in the PFC that may be linked to persons with ASD include atypical cortical growth patterns, deviations in cortical thickness, and dysregulation of neurons and their connections to other brain regions. In cases of ASD, the PFC has an atypical increase in size throughout the early years after birth. Either normalization or a reduction in volume will occur as a result of this excessive expansion of the PFC. A study discovered a rise in the cortical thickness throughout childhood in individuals with ASD, which then returned to normal levels in later stages of life. An estimated 67 % increase in the total number of neurons in the PFC was seen in patients with ASD. Patients with ASD exhibit a notable decrease in the size of pyramidal neurons in the PFC, indicating a disruption in long-distance communication. The mouse model's medial PFC showed an increase in the ratio of excitatory to inhibitory cellular activity, resulting in impairments in social behaviors (Donovan & Basson, 2017; Varghese et al., 2017).

ASD instances have changes in the anatomy of the hippocampus, including alterations in hippocampal volume, shape, and aberrant textural features. Research using task-based functional magnetic resonance imaging has established a connection between the hippocampus and deficits in learning and memory, perception of social emotions, and heightened sensitivity to sensory stimuli in individuals with ASD. Furthermore, certain research indicates that persons with ASD experience difficulties in establishing relationship representations, resulting in more pronounced ASD symptoms and less connection between the hippocampus and the caudate nucleus. These impairments are likely attributed to defects in cognitive mapping (Banker et al., 2021). An *in vitro* study has detected alterations in the number of Purkinje cells and the occurrence of cerebellar atrophy, as well as abnormalities in the activity of the temporal lobe and delayed development of sensorimotor skills in individuals with ASD. The researchers hypothesized that the medial PFC and the hippocampus are the brain regions most impacted by ASD. Pyramidal cell depletion in the CA1 and CA3 regions of the hippocampus has been observed in the rat model of autism. The primary cause of an imbalance between excitatory and inhibitory signals in the same model is the dysregulation of the GABAergic system, which involves a reduction in the number of GABAergic interneurons and reduced GABAergic neurotransmission (Bódi et al., 2022).

NF- $\kappa$ B facilitates the activation of pro-inflammatory cytokines, including TNF- $\alpha$ , IL-1, and IL-6. Long non-coding RNAs (lncRNAs) associated with NF- $\kappa$ B may contribute to the development of ASD and can serve as diagnostic indicators for ASD (Tamizkar et al., 2021). The higher expression of IL-6 suggests a potential involvement of this cytokine in the development of ASD. The levels of IL-6 are elevated in the cerebellum of individuals with ASD, and this leads to alterations in the adhesion and migration of neurons, as well as the regulation of synapse growth (Wei et al., 2011). It is worth mentioning that the analysis of cytokines has identified TNF- $\alpha$  as a significant cytokine that is not functioning properly in individuals with ASD (Xie et al., 2017).

Glutathione peroxidase (GSH-Px) is a crucial cellular antioxidant that safeguards neural cells against oxidative harm. Multiple studies have demonstrated a reduction in GSH-Px activity in the cerebellum, erythrocytes, and plasma in individuals with ASD. This leads to a weakness in antioxidant defense systems. A separate study found that the activity of brain GSH-Px decreased in autism rodent model. Conversely, certain studies have observed a rise in plasma GSH-Px activity among autistic children (Bjørklund et al., 2020).

The specific neuropathological alterations in the noradrenergic system in individuals with ASD are not yet fully understood. Preliminary findings suggested that persons with ASD who received treatment with  $\beta$ -adrenergic antagonists, such as propranolol, saw enhancements in their linguistic and social behaviors. This improvement is attributed to the increased functional connectivity induced by the medication. Propranolol has the potential to be a beneficial treatment for emotional, behavioral, and autonomic dysfunction in individuals with ASD.  $\alpha$ 2 adrenergic agonists, which suppress the release of noradrenaline (NA) neurons, have demonstrated efficacy in improving hyperactivity, impulsivity, hyperarousal, and social connections in individuals with ASD, as observed in double-blinded placebo-controlled crossover experiments. Multiple studies have shown heightened noradrenergic activity in individuals with ASD, as seen by elevated levels of epinephrine and norepinephrine in the blood plasma, as well as abnormal excretion of different catecholaminergic metabolites in urine (Beversdorf et al., 2021).

The firing of noradrenergic neurons in the hindbrain cDVC, namely the A2 neurons, has been found to play a role in regulating various crucial physiological processes, including learning, memory, and emotional and cognitive events (Rinaman, 2011). Nevertheless, it remains uncertain whether the disruption of A2 noradrenergic release has a role in the neurodevelopmental dysfunction observed in individuals with ASD.

Thus, in this investigation, we postulated that depleting NA via inhibiting the caudal cDVC hindbrain A2 neurons could modify the inflammatory activity in the animal model of ASD. This study aims to investigate the impact of inhibiting cDVC hindbrain A2 neurons with 6-OHDA on the hippocampus and PFC in the presence of systemic LPS-induced neuroinflammation in the VPA-autistic animal model. The study will primarily focus on three aspects: a. Assessing the behavior of the animals. b. Measuring the gene expression of inflammatory cytokines, specifically IL-6, TNF- $\alpha$ , and NF- $\kappa$ B, by utilizing qRT-PCR. c. Measuring the protein expression of inflammatory and oxidative stress markers, including COX-2, GPX-1, p-AMPK, and AMPK, using western blot analysis.

## 2. Materials and methods

### 2.1. Materials

VPA was obtained from Sigma-Aldrich (Saint Louis, MO, United States of America (USA)). 6-OHDA, L-ascorbic acid and LPS were obtained from (Medchemexpress, USA). Ketamine and xylazine was obtained from Prince Naif bin Abdul-Aziz Health Research Center, King Saud University (KSU), Saudi Arabia (SA). Optimal Cutting Temperature (OCT) was obtained from (ThermoFisher Scientific, USA). Trizol reagent was obtained from (Invitrogen, USA). SYBR Green, PCR Master Mix, and cDNA reverse transcription kit were bought from (Medchemexpress, USA). IL-6, TNF- $\alpha$ , and NF- $\kappa$ B primers were created and customized by (integrated DNA Technologies (IDT), Belgium). Cocktail protease inhibitors and RIPA lysis buffer were purchased from (ThermoFisher Scientific, USA). Bicinchoninic acid assay (BCA assay) was purchased from (Molequle-on, Auckland, New Zealand). Primary rabbit polyclonal antibodies COX-2, GPx-1, p-AMPK, AMPK, and GAPDH and secondary horseradish peroxidase goat antirabbit IgG antibodies were purchased from (ABclonal Technology, USA).

### 2.1.1. Experimental models

These experiments were performed using male Sprague-Dawley (SD) rats (6 – 8 weeks - old, weighing 100–180 g) which were obtained and housed with free access to standard animal needs of food and water during the experiment (23 °C and a 12 h light/dark cycle) at Prince Naif bin Abdul-Aziz Health Research Center, the animal laboratory center, KSU, SA. Institutional Animal Care Experiment Ethics Committee (IACUC) approval was approved by the research ethics committee at King Saud University on December 19, 2021 (reference number: KSU-SE-21–79).

## 2.2. Methods

### 2.2.1. Study design

#### 2.2.1.1. Induction of autism-like behaviors using valproic acid (VPA) model.

Firstly, an autism-like behaviors model in SD rats was induced through the animal center breeding protocol (1 male: 2 females) in each cage. The pregnancy was identified by the vaginal plug, and the rats were separated into different cages. Then, pregnant SD rats were injected with VPA 500 mg/kg (or saline) as i.p. on gestational day (GD) 12.5, and VPA was dissolved in 250 mg/ml of saline. (Nicolini & Fahnestock, 2018; Favre et al., 2013; Servadio et al., 2018). After 21 post-natal days (PND), the pups were divided into groups to conduct the remaining treatment stage. The VPA-induced autism-like behavioral model exhibited developmental defects, including alopecia (hair loss), tail deformity, and delayed weight growth rate. These findings were previously established in a study by Ruhela et al. (2019). The VPA model's autism-like behavior was validated by assessing repetitive behaviors using a self-grooming test and marble-burying test on PND 30 – 40. All male rats that exhibited autism-like behavior after prenatal exposed to VPA were included in further stereotaxic surgery and treatment.

On PND 45, the animals were anesthetized using Ketamine 90 mg / 10 mg xylazine/ml (i.p.) based on the rat weight (0.1 ml/100 g) (Butler Schein, Inc., Melville, NY, USA). During the initial day of the experiment, the animals underwent a brain stereotaxic surgery in which a PE20 cannula was inserted into the caudal fourth ventricle (CV4). The coordinates for the insertion were determined to be 0 mm lateral to the midline, 13.3 mm posterior to bregma, and 6.6 mm ventral to the surface of the skull (Alhamami et al., 2018). After the surgery, the animals transferred into separate cages and the health of each rat until was monitored drug treatment. On PND 52–54, after the recovery period, the animals were injected with drugs either icv, into the hindbrain CV4 or i. p. at 9.00 a.m. as following four treatment groups: Group I (Positive-controlled): 6 VPA- treated rats (autistic Animal model) were treated by vehicle (0.2 % ascorbic acid diluted with 0.9 % sterile saline-injected (icv), into CV4 and VEH (saline 0.9 % NaCl, i.p.). Group II: 6 VPA-treated rats were injected by (75 µg/µl/day) 6-OHDA (icv), into CV4 twice (one day apart from another) (Alhamami et al., 2018), and VEH (saline 0.9 % NaCl, i.p.). Group III: 6 VPA- treated rats were injected by VEH (saline 0.9 % NaCl) (icv), into CV4 and LPS (500 µg/kg - i.p.) (Zhao et al., 2019) - (Wang et al., 2017), (LPS was injected at PND 54 as positive group for neuroinflammation). Group IV: 6 VPA- treated rats were injected by (75 µg/µl/day) 6-OHDA (icv), into CV4 twice (one day

**Table 1**  
Experimental Groups Treatment.

Group	Treatment
VPA - Positive controlled	0.2 % ascorbic acid / 0.9 % saline-injected icv, into (CV4) + VEH (saline 0.9 % NaCl - i.p.).
VPA - 6-OHDA	(75 µg/µl/day) 6-OHDA through CV4 <b>twice</b> (one day apart from another) + VEH (saline 0.9 % NaCl - i.p.).
VPA - LPS	VEH (saline 0.9 % NaCl) into CV4 + LPS (500 µg/kg - i.p.).
VPA - 6-OHDA + LPS	(75 µg/µl/day) 6-OHDA through CV4 <b>twice</b> (one day apart from another) + LPS (500 µg/kg - i.p.).

apart from another), and LPS (500 µg/kg - i.p.), (LPS was injected on PND 54).

The self-grooming test was performed on PND 54–55 for repetitive behavioral assessment after drug treatments. On PND 55, rats were anesthetized by ketamine/xylazine mixture as i.p., then the brain tissue was harvested and collected in the liquid nitrogen-cooled isopentane at 11.00p.m. Also, blood was collected in a tube immediately from the orbital sinus, and the plasma was separated for future analysis (chart 1). The brain and plasma samples were stored at –80 °C for molecular experiments.

### 2.2.2. Repetitive behavioral assessments: Self-grooming test and marble burying test

Repetitive behavior is one of the core symptoms associated with ASD, and VPA rats expressed these repetitive behaviors (Hirsch et al., 2018; Zamberletti et al., 2019). Repetitive behavior in the SD prenatal rats was assessed using the self-grooming test. In this experiment, animals were placed in a sterile empty cage (26 cm x 48 cm x 20 cm) to adapt to the area for 10 mins. After the habituation period, the self-grooming activity will be scored manually by the stopwatch for another 10 mins. The grooming activity that was addressed in this experiment includes body grooming, head washing, genital tail grooming, and leg-licking.

VPA rats expressed more immersed marble numbers than the control group, and this repetitive behavior was determined using the marble burying test (Scheggi et al., 2020). Firstly, fresh and unscented bedding of 5 cm in depth was added to clean the polycarbonate cage (26 cm x 48 cm x 20 cm). Then, 20 standard glass marbles were arranged on the surface of the bedding in parallel lines as four columns and five rows. After that, individual rats were placed in the same cage corner, and the number of marbles buried recorded after 30 min of the test. The used marbles were always washed in laboratory detergent, rinsed with distilled water, and dried before each use (Angoa-pérez et al., 2013).

### 2.3. Tissue cryo-sectioning

Cryostat-sectioning is a method to isolate the area of interest in the frozen brain tissues. After isolating brain tissue from rats, samples were stored at –80 °C. Then, the brain was separated into the fore and hindbrain parts. Then, the frozen tissue was put on the Cryostat mold (Leica CM1800, USA) that was embedded with OCT (ThermoFisher Scientific, USA). After that, the mold that contained tissue was returned into a freeze frame on the apparatus. Then, the suitable position was adjusted for the sectioning of brain tissue. Then, sectioning brain tissue was performed until forebrain regions such as PFC or hippocampus were reached based on the rat brain atlas. PFC area is characterized by two connected curved lines and two spots. When the PFC was reached, its tissues were isolated using a blade to a 1.5 ml tube. Then, the sectioning was kept until we reached the hippocampus, characterized by the banana shape, which was isolated by the blade to the tube. Finally, PFC and hippocampus samples were stored at –80 °C for molecular experiments.

### 2.4. Quantitative Real-Time polymerase chain reaction qRT-PCR

Total RNA was isolated from animal tissues using TRizol reagent. cDNA was obtained from the reverse transcription of the sample RNA using a cDNA reverse transcription kit (Medchemexpress, USA). Forward and reverse primers for target genes (Table 2) were gained from Integrated DNA Technology, USA. The PCR findings were represented by the cycle threshold (CT) value, which indicated the number of cycles needed for the fluorescent signal to reach the threshold. The relationship is inverse between the quantity of the gene of interest in the samples and the expression of the GAPDH housekeeping gene. The gene with a higher expression level is associated with a lower CT value, and vice versa. The fold difference was calculated using the 2- $\Delta\Delta$ CT method.

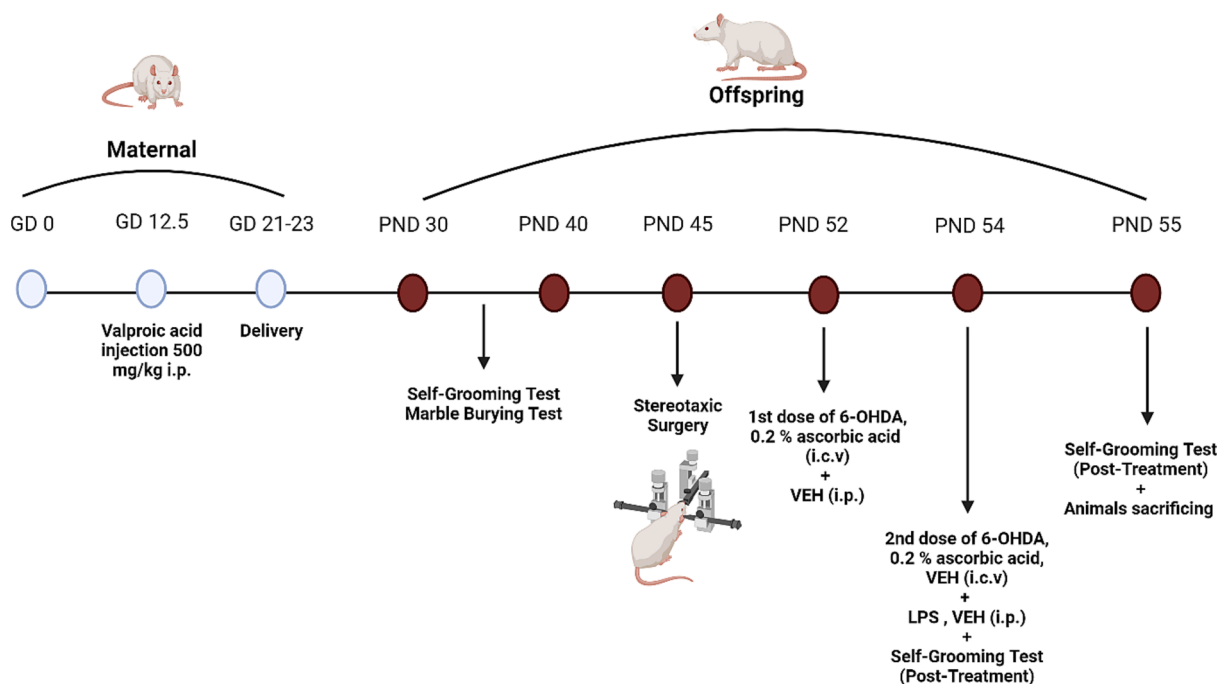


Chart 1. Experimental Protocol of Animal Treatment.

Table 2

List of genes primers used in PCR.

Gene	Primer sequence
IL-6	FR: 5'-TCCTACCCCAACTTCCAATGCTC-3'
	RP: 5'-TTGGATGGTCTTGGTCCTTAGCC-3'
TNF- $\alpha$	FR: 5'-AAATGGGCTCCCTCTCATCAGTTC-3'
	RP: 5'-TCTGCTTGGTGGTTTGCTACGAC-3'
NF- $\kappa$ B	FR: 5'-CGCAAAGGACCTACGAGAC-3'
	RP: 5'-TGGGGGAAAACCTCATCAAAG-3'
GAPDH	FR: 5'-TGCCAGCCTCGTCTCATAG-3'
	RP: 5'-ACTGTGCCGTTGAACCTGC-3'

Table 2. IL-6 (Interleukin-6), TNF- $\alpha$  (Tumor Necrosis Factor Alpha), NF $\kappa$ B (nuclear transcription factor kappa B), and GAPDH (Glyceraldehyde-3-Phosphate Dehydrogenase)

## 2.5. Western blot analysis

Firstly, protein was isolated from tissues (the PFC& hippocampus) in 2 ml tube through a homogenization process using 30–40 mg of tissue in an ice-cold box in 400  $\mu$ l RIPA lysis buffer mixed with 4  $\mu$ l of protease and phosphatase inhibitor cocktail (Santa Cruz Biotechnology, USA). Protein lysates were incubated for 1 h on ice, and samples were vortexed every 15 min, followed by centrifuging at 12,000 rpm for 15 min at 4  $^{\circ}$ C. After that, supernatants of samples were collected into 1.5 ml tube and stored at -20  $^{\circ}$ C for further experiments. The protein concentration for each sample was quantified using the e bicinchoninic acid assay (BCA) method for protein concentration estimation. (Molecule on, Auckland, New Zealand).

After that, sample proteins were mixed with distilled water and 2x Laemmli sample buffer to use this mixture in a western blot run (Santa Cruz Biotechnology, USA). Then, samples were denatured by heating at 50  $^{\circ}$ C for 5–10 min. Sodium dodecyl sulfate–polyacrylamide gel electrophoresis (SDS-PAGE) was used to separate proteins by mass and charge from the negative to the positively charged electrode through the gel. Gels were prepared in two layers, resolving gel and stacking gel. Then, 2.5–5  $\mu$ l of the ladder was loaded in the first lane to help in identifying the molecular weight for the protein of interest, and 25–30  $\mu$ g of protein samples per lane was loaded on 10–12.5% SDS-polyacrylamide gel at 110 V for 70–80 min. After that, proteins were

transferred into nitrocellulose membranes (Santa Cruz Biotechnology, USA) using a semi-dry transfer instrument at 18 V for 1 h (Bio-Rad, USA). The membrane was blocked with bovine serum albumin (BSA) in a washing buffer (TBST) for 1–2 h. The membrane was then incubated overnight on the saker with rabbit polyclonal antibodies against COX-2 (1:2000), GPx-1 (1:1000), p-AMPK (1:1000), AMPK (1:1000), and GAPDH (1:10000) protein at 4  $^{\circ}$ C (ABclonal Technology, USA). The next day, membranes were washed 3–5 times with TBST for 5 min. After that, membranes were incubated with fresh peroxidase-conjugated goat anti-rabbit HRP IgG antibody (1:10000) (ABclonal Technology, USA) for 1–2 h. Then, membranes were washed every 5 min 3–5 times with TBST. Proteins band expressions were visualized based on the standard protein ladder through the ChemiDoc MP imaging system (Bio-Rad, USA) using a western blotting luminol reagent (1000  $\mu$ l: 1000  $\mu$ l) (Santa Cruz Biotechnology, USA). Finally, ImageJ software was used to analyze the expression bands, and the resulting data was imported into Microsoft Excel for fold change calculation.

## 2.6. Statistical analysis

Each experiment was conducted on at least three biological replicates. The data were presented as mean of standard error  $\pm$  SEM and defined as  $P$ -value ( $<0.05$ ). Treated groups were compared by unpaired T-test and one-way analysis of variances (ANOVA) followed by the Tukey post hoc test. The statistical analyses and figures were performed using Graph Pad Prism version 10.1.

## 3. Results

### 3.1. The validity of VPA induction of Autism-Like behaviors

#### 1. Prenatal exposure to VPA increases self-grooming behaviors

Changes in repetitive behaviors of VPA rats were assessed to validate that the prenatal exposure of VPA induced autism-like behaviors with a comparison to untreated (healthy) male rats. VPA-treated rats showed more spending time (sec.) in the self-grooming test, significantly compared to the untreated healthy group (Fig. 1A).

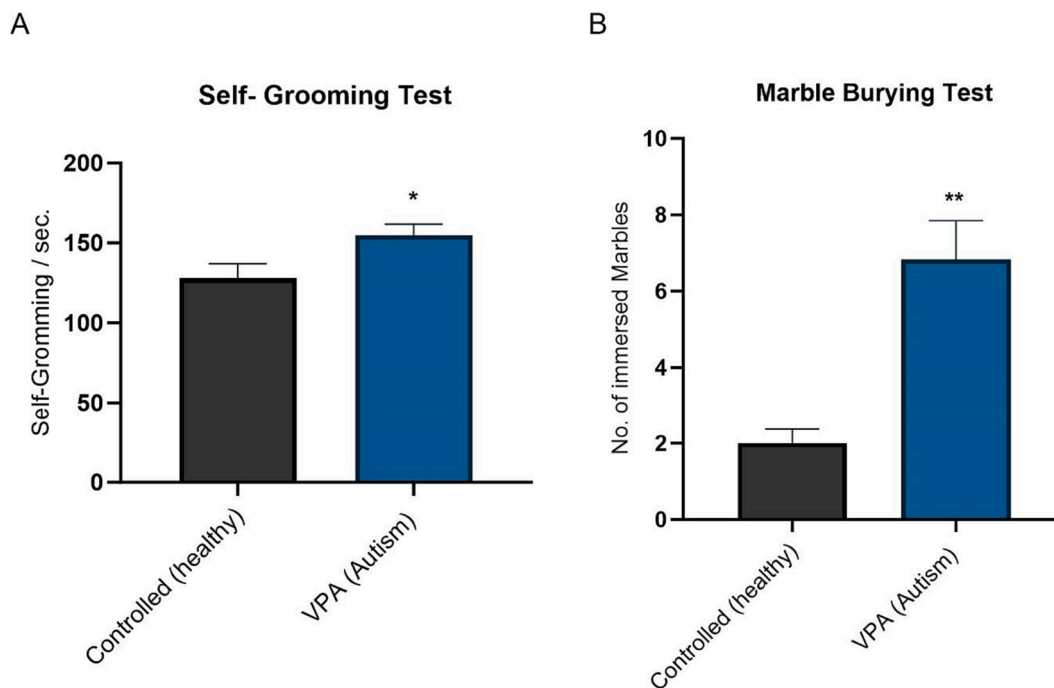


**Fig. 1.** Behavioral tests. A) prenatal exposure to VPA increases self-grooming behaviors. Data are shown as the mean  $\pm$  SEM ( $n = 6$ ) and considered statistically significant with  $*P < 0.05$ . B) prenatal exposure to VPA increases marbles behaviors.. Pregnant SD rats were injected with VPA 500 mg/kg i.p. on GD 12.5, and VPA was dissolved in 250 mg/ml of saline. Data expressed as the mean  $\pm$  SEM ( $n = 6$ ) with  $**P < 0.01$  considered statistically significant.

## 2. Prenatal exposure to VPA increases immersed marbles behaviors

Altered repetitive behaviors of VPA rats were assessed in a marble burying test to validate that prenatal exposure of VPA induced autism-like behaviors compared to untreated (healthy).

male rats. VPA-treated rats exhibited more repetitive behaviors by increasing the number of immersed marbles more significantly compared to the untreated healthy group (Fig. 1B).

### 3.2. The effect of 6-OHDA and LPS on the Self-Grooming behavior of the VPA autism model

Repetitive behavior changes of VPA rats, especially (self-grooming), were assessed after animal treatment according to the study design protocol. VPA animal model that was treated with (VEH-saline 0.9 % NaCl - icv. + LPS 500  $\mu$ g/kg - i.p.) showed more spending time (sec.) in the self-grooming test significantly compared to the VPA-controlled group. Self-grooming spending time was increased in the combination group (6-OHDA 75  $\mu$ g/ $\mu$ l/day icv. + LPS 500  $\mu$ g/kg - i.p.) more significantly compared to VPA-controlled group. The self-grooming behaviors of VPA animals that were treated with 6-OHDA 75  $\mu$ g/ $\mu$ l/day icv. showed no significant difference compared to other treatment groups of study (Fig. 2).

### 3.3. The effect of 6-OHDA and LPS treatment on the inflammatory Gene's expression at the PFC area of the VPA-Autism model

#### 1. NF- $\kappa$ B, IL-6 and TNF- $\alpha$ Gene Expression at the PFC

Inflammatory markers such as NF- $\kappa$ B, IL-6 and TNF- $\alpha$  are used in the molecular field to indicate the neuro-inflammation of SD rats. So, the gene expression level of these markers at the PFC area of the VPA-autism model was assessed using the qRT-PCR technique. VPA-autism animals treated with (6-OHDA 75  $\mu$ g/ $\mu$ l/day icv. + VEH-saline 0.9 % NaCl i.p.) showed significant induction of NF- $\kappa$ B gene expression at PFC compared to VPA-controlled group. NF- $\kappa$ B gene expression level at the PFC area in

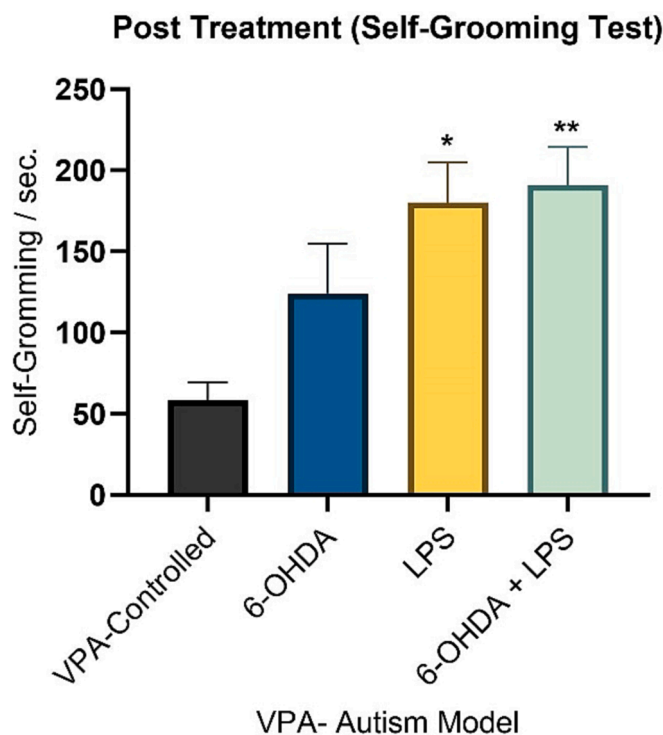


**Fig. 2.** 6-OHDA and LPS increases self-grooming behaviors in VPA autism model. The self-grooming test was used to evaluate the changes of repetitive behaviors between VPA-SD rats animals' treatment. Data are shown as the mean  $\pm$  SEM ( $n = 4$ ) and considered statistically significant with  $*P < 0.05$  (VPA-controlled Vs LPS) and  $**P < 0.01$  (VPA-controlled Vs 6-OHDA + LPS).

VPA autism animals that were treated with (VEH-saline 0.9 % NaCl - icv. + LPS 500  $\mu$ g/kg - i.p.) was significantly increasing compared to VPA-controlled group. VPA-autism animals treated with the

combination group (6-OHDA 75 µg/µl/day icv. + LPS 500 µg/kg i.p.) showed significant induction of NF-κB gene expression level at the PFC area compared to VPA-controlled group (Fig. 3A).

In order to evaluate the effect of 6-OHDA after LPS-induced neuro-inflammation of the VPA autism model, the IL-6 gene expression level at the PFC area of VPA-autism animals was assessed using the qRT-PCR technique. VPA-autism animals treated with (6-OHDA 75 µg/µl/day icv. + VEH-saline 0.9 % NaCl i.p.) showed significant induction of IL-6 gene expression at PFC compared to VPA-controlled group. IL-6 gene expression level at the PFC area in VPA autism animals that were treated with (VEH-saline 0.9 % NaCl - icv. + LPS 500 µg/kg - i.p.) was significantly increased compared to VPA-controlled group. VPA-autism animals treated with the combination group (6-OHDA 75 µg/µl/day icv. + LPS 500 µg/kg - i.p.) showed significant reduction of IL-6 gene expression level at the PFC area compared to 6-OHDA group (Fig. 3B).

The TNF-α gene expression level at the PFC area of VPA-autism animals was assessed using the qRT-PCR technique to clarify the effect of 6-OHDA after the LPS-induced neuro-inflammation of the VPA autism model. VPA-autism animals treated with (6-OHDA 75 µg/µl/day icv + VEH-saline 0.9 % NaCl i.p.) showed significant induction of TNF-α gene expression at PFC compared to VPA-controlled group. TNF-α gene expression level at the PFC area in VPA autism animals that were treated with (VEH-saline 0.9 % NaCl - icv. + LPS 500 µg/kg - i.p.) was significantly decreasing compared to the 6-OHDA group. VPA-autism animals treated with the combination group (6-OHDA 75 µg/µl/day icv. + LPS 500 µg/kg i.p.) showed a significant reduction of TNF-α gene expression level in the PFC area compared to 6-OHDA group (Fig. 3C).

## 2. NF-κB, IL-6, and TNF-α Gene Expression at the hippocampus

NF-κB gene expression at the hippocampus area in the VPA-autism model was assessed using qRT-PCR. VPA-autism animals treated with the combination treatment group showed slightly induction of NF-κB gene expression level at the hippocampus compared to controlled group. The data did not show any significant difference between treatment groups of the study (Fig. 4A).

The IL-6 gene expression level at the hippocampus area of the VPA-autism model was assessed using the qRT-PCR technique. The IL-6 gene expression level was significantly decreased in VPA treated with the combination group (6-OHDA 75 µg/µl/day icv. + LPS 500 µg/kg i.p.)

compared to the LPS group. The data did not show a significant difference between other treatment groups of the study (Fig. 4B).

TNF-α gene expression at the hippocampus area in the VPA-autism model was assessed using qRT-PCR. VPA autism animals that were treated with (VEH-saline 0.9 % NaCl - icv. + LPS 500 µg/kg - i.p.) showed significant induction of TNF-α gene expression at hippocampus area compared to VPA-controlled group. The data did not show any significant difference between other treatment groups of the study (Fig. 4C).

## 3.4. The effect of 6-OHDA and LPS treatment on the Protein's expression of inflammatory and oxidative stress markers at the PFC area in the VPA-Autism model

### 1. COX-2 and GPX-1 Protein Expression at the PFC

The protein expression level of the COX-2 marker at the PFC area of the VPA-autism model was assessed using the western blot technique. VPA-autism animals treated with (VEH-saline 0.9 % NaCl - icv. + LPS 500 µg/kg - i.p.) showed significant induction of COX-2 protein expression at PFC compared VPA-controlled and 6-OHDA groups, respectively. The data did not show any significant difference between other treatment groups of the study (Fig. 5A, 5C).

The protein expression level of the GPX-1, which is an oxidative stress marker, at the PFC area of the VPA-autism model was determined using the western blot technique. VPA-autism animals treated with (VEH-saline 0.9 % NaCl - icv. + LPS 500 µg/kg - i.p.) showed a significant reduction of the GPX-1 protein expression level at PFC compared to VPA-controlled group. GPX-1 protein expression level at the PFC area in VPA autism animals that were treated (6-OHDA 75 µg/µl/day icv. + LPS 500 µg/kg i.p.) was significantly decreased compared to VPA-controlled group. The data did not show any significant difference between other treatment groups of the study (Fig. 5B, D).

### 2. The effect of 6-OHDA and LPS treatment on the p-AMPK and AMPK protein's expression at the PFC area in the VPA-autism model.

The protein expression level of p-AMPK and AMPK at the PFC area of the VPA-autism model was detected using the western blot technique. The data showed no significant differences between all treatment groups

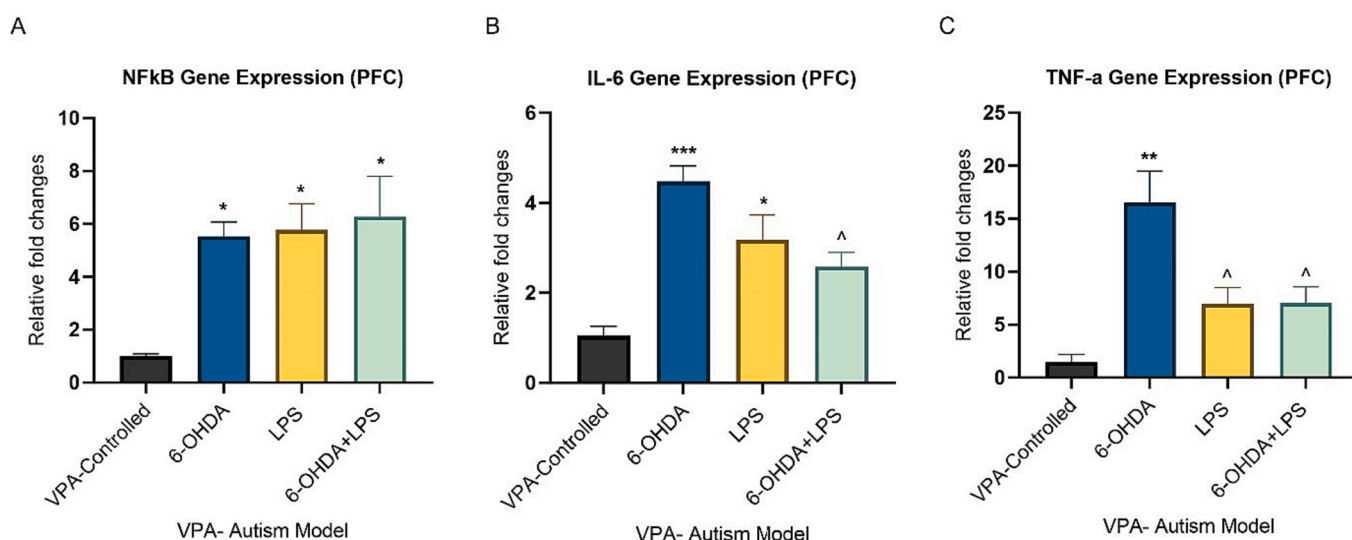


**Fig. 3.** The effect of 6-OHDA and LPS treatment on A) NF-κB, B) IL-6, and C) TNF-α gene expression at PFC area in VPA-autism model. RNA samples were analyzed using qRT-PCR technique. Fig. 3A data are shown as the mean ± SEM (n = 3) and considered statistically significant with \*P < 0.05 (VPA-controlled Vs 6-OHDA, LPS and 6-OHDA + LPS). Fig. 3B data are shown as the mean ± SEM (n = 3) and considered statistically significant with \*P < 0.001 (VPA-controlled Vs 6-OHDA), \*P < 0.05 (VPA-controlled Vs LPS) and \*P < 0.05 (6-OHDA Vs 6-OHDA + LPS). Fig. 3C data are shown as the mean ± SEM (n = 3) and considered statistically significant with \*\*P < 0.01 (VPA-controlled Vs 6-OHDA) and \*P < 0.05 (6-OHDA Vs LPS and 6-OHDA + LPS).

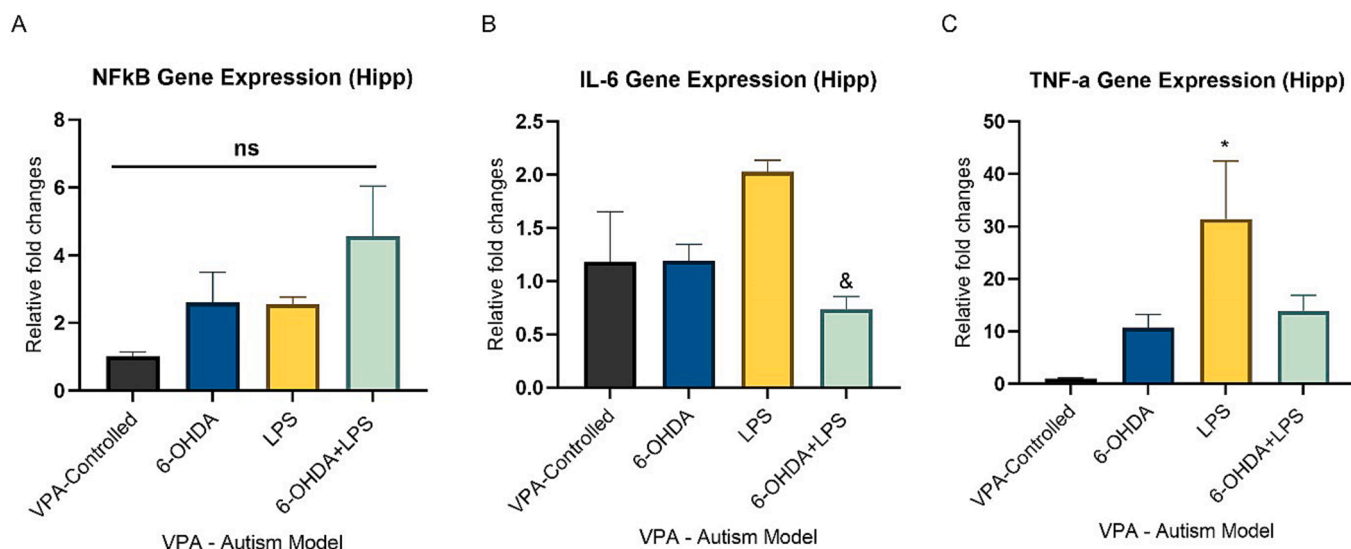


**Fig. 4.** The effect of 6-OHDA and LPS treatment on A) NF- $\kappa$ B, B) IL-6, and C) TNF- $\alpha$  gene expression of at hippocampus area in VPA-autism model. RNA samples were analyzed using qRT-PCR technique. Fig. 4A data are shown as the mean  $\pm$  SEM (n = 3). Fig. 4B data are shown as the mean  $\pm$  SEM (n = 3) and considered statistically significant with  $\&P < 0.05$  (LPS Vs 6-OHDA + LPS). Fig. 4C data are shown as the mean  $\pm$  SEM (n = 3) and considered statistically significant with  $*P < 0.05$  (VPA-controlled Vs LPS).

in p-AMPK (Fig. 6A, 6C) as well as in AMPK (Fig. 6B, D) protein expression levels at PFC compared to each other's.

The Effect of 6-OHDA and LPS Treatment on the Protein's Expression of Inflammatory and Oxidative Stress Markers at the hippocampus area in the VPA-Autism Model.

#### 1. COX-2 and GPX-1 protein expression at the hippocampus

The protein expression level of the COX-2 marker at the hippocampus area of the VPA-autism model was assessed using the western blot technique. COX-2 protein expression level at the hippocampus area in VPA autism animals that were treated with (VEH-saline 0.9 % NaCl - icv. + LPS 500  $\mu$ g/kg - i.p.) was significantly increased compared to 6-OHDA group. The data has shown no significant differences between other groups of treatment. (Fig. 7A, C).

The oxidative stress marker, such as GPX-1, was used to indicate the oxidant/antioxidant activity in SD rats. So, the protein expression level of the GPX-1 marker at the hippocampus area of the VPA-autism model was obtained using the western blot technique. VPA-autism animals treated with (VEH-saline 0.9 % NaCl - icv. + LPS 500  $\mu$ g/kg - i.p.) showed a significant reduction of the GPX-1 protein expression level at the hippocampus compared to VPA-controlled group, and 6-OHDA group, respectively. The data has shown no significant differences between other groups of treatment. (Fig. 7B, D).

#### 2. The effect of 6-OHDA and LPS treatment on the p-AMPK and AMPK protein's expression at the hippocampus area in the VPA-autism model.

The protein expression level of p-AMPK and AMPK at the hippocampus area of the VPA-autism model was gained using the western blot technique. The data showed no significant differences between all treatment groups in p-AMPK (Fig. 8A, C) as well as in AMPK (Fig. 8B, D) protein expression levels at the hippocampus compared to each other's.

#### 4. Discussion

ASD is a neurodevelopmental disorder that is typically diagnosed during early childhood (Lord et al., 2020). The worldwide prevalence rate of ASD is around 1 in 100 children, according to Zeidan et al.

(2022). ASD affects males nearly four times more than females (Maenner et al., 2023). We expect that the female brain will respond differently to this disorder due to the presence of estradiol at much higher levels than in males, as estradiol has played an important role in brain sex-specific difference responses to several types of stressors, such as low blood glucose levels (Briski et al., 2018). ASD is classified as a polygenic condition that arises from the interplay between genetic and environmental variables (Park et al., 2016). The precise pathophysiology of ASD remains uncertain due to its intricate nature. Several potential explanations, including impaired immunity and neuroinflammation, have been suggested to elucidate the etiology of ASD (Yenkoyan et al., 2017). CNS NA plays a distinct role in mitigating and slowing down the advancement of certain neurological disorders. Several research have indicated that NA exhibits an anti-inflammatory impact in both in-vivo and in-vitro investigations (O'Sullivan et al., 2008). Our work examined the impact of depleting the hindbrain cDVC A2 NA neurons injecting the 6-OHDA icv. in the PFC and hippocampus in VPA-autistic animal models. In addition, LPS i.p. was administered to further examine the effect in those regions under the condition of LPS-driven neuroinflammation.

The rat model of valproic acid is an environmentally induced model that exhibits robust construct and clinical validity. The basis of this is the teratogenicity of VPA in humans, which refers to the ability of VPA to cause birth defects. When mothers are treated with VPA during the early stages of pregnancy, there is a higher likelihood of giving birth to a child with autism. the dose used in this study was approved to induce an animal-autistic model according to many references, including Nicolini & Fahnestock, 2018, Favre et al., 2013, and Servadio et al., 2018. In addition, we avoid using other high doses of VPA, which can lead to a high fetal reabsorption rate and increased animal deaths.

Repetitive behaviors are fundamental symptoms linked to ASD, and rats treated with VPA exhibited these repetitive behaviors. The autism-like behaviors generated by VPA was confirmed by evaluating repetitive activities such as self-grooming and marble-burying tests. Our data indicated that prenatal exposure to VPA resulted in increased time spent on body grooming (in seconds) (Fig. 1A) and a substantial increase in the number of marbles immersed compared to healthy control rats (Fig. 1B). Consistent with this discovery, prior research that used VPA to trigger autistic-like behaviors observed that this autism model had considerably higher levels of repeated behaviors in both self-grooming and marble-

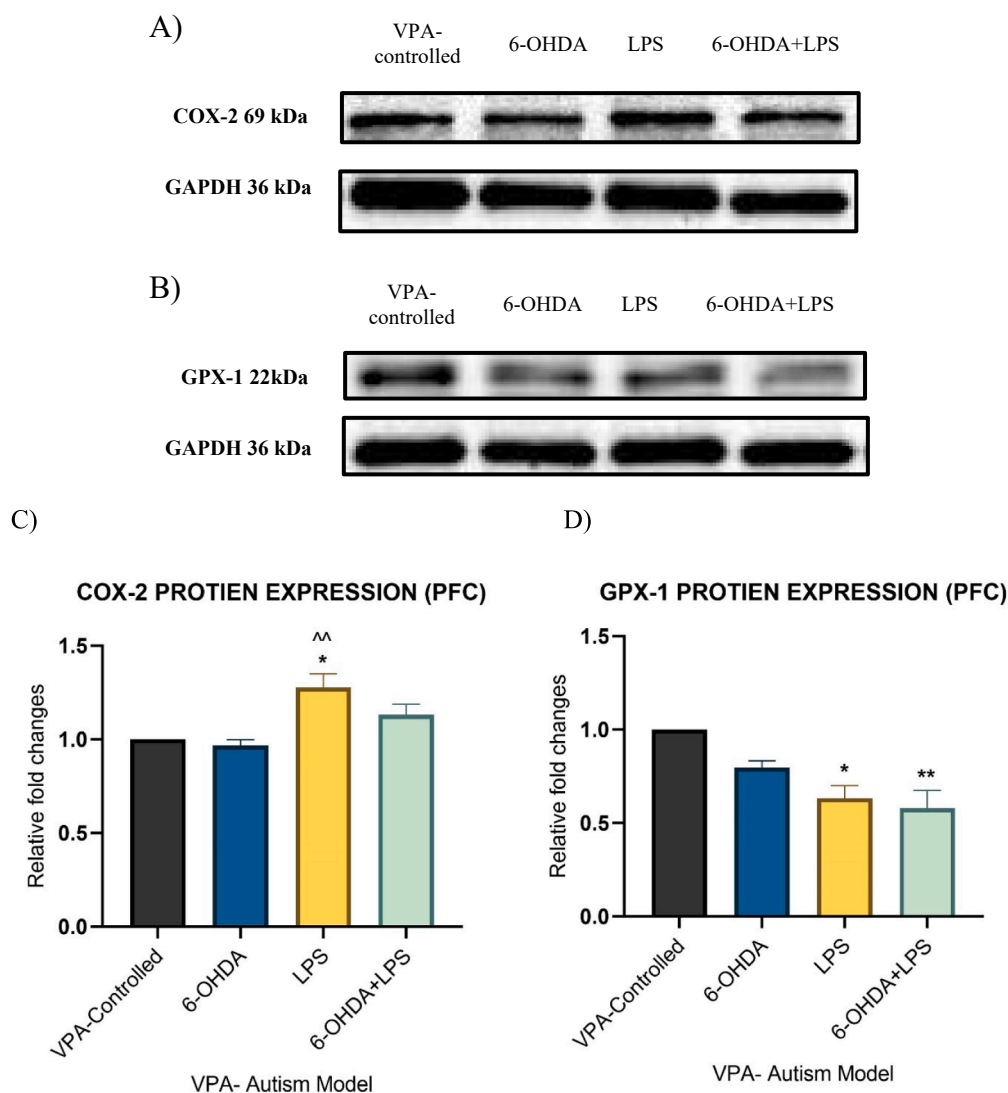


**Fig. 5.** The effect of 6-OHDA and LPS treatment on A) COX-2 and B) GPX-1 protein expression at PFC area in VPA-autism model. (A) COX-2 Protein samples were analyzed using western blot technique. GAPDH was used as loading control. (C) represented relative changes in the level of COX-2 protein compared to controlled group. (B) GPX-1 Protein samples were analyzed using western blot technique. GAPDH was used as loading control. (D) represented relative changes in the level of GPX-1 protein compared controlled group. Fig. 5A-C data are shown as the mean  $\pm$  SEM (n = 3) and considered statistically significant with \*P < 0.05 (VPA-controlled Vs LPS) and <sup>\*\*</sup>P < 0.01 (6-OHDA Vs LPS). Fig. 5B-D data are shown as the mean  $\pm$  SEM (n = 3) and considered statistically significant with \*P < 0.05 (VPA-controlled Vs LPS) and <sup>\*\*</sup>P < 0.01 (VPA-controlled Vs 6-OHDA + LPS).

burying tests compared to the control group (Zamberletti et al., 2019; Scheggi et al., 2020).

Furthermore, the repetitive self-grooming behavior of the VPA-autism model following the animals' treatment was evaluated based on the experimental study design outlined in Table 1. Our data indicated that the VPA animal model, which received VEH-saline icv. + LPS i.p. treatment exhibited a substantial increase in the duration (in seconds) of self-grooming during the repetitive behaviors test compared to the VPA-controlled group. This finding suggests that the intraperitoneal administration of LPS in the VPA autism model can enhance the manifestation of autistic-like behaviors in the VPA model. The findings align with prior in-vivo research indicating that LPS injections can activate microglia by triggering the NF- $\kappa$ B signaling pathway. Additionally, LPS injections can result in increased neuronal cell death, which can subsequently contribute to cognitive impairment (Zhao et al., 2019). The combined group of 6-OHDA icv. + LPS i.p. showed a considerably higher increase in self-grooming time compared to the VPA-controlled group. The self-grooming behaviors of animals treated with icv. 6-OHDA alone

exhibited reduced time spent on self-grooming in comparison to the LPS or combination groups. This study is the first to examine the impact of CV4 6-OHDA icv administration, either alone or in combination with LPS i.p., on any animal autistic model. A study has shown that 6-OHDA can cause anxiety-like behaviors in rats with Parkinson's disease (PD). As discussed before, anxiety is one of the illnesses that can be linked to ASD (Vieira et al., 2019; Oliynyk et al., 2023). The findings of our study suggest that the combined treatment of 6-OHDA and LPS resulted in a more pronounced increase in VPA-induced autism-like behaviors compared to the control group. This effect was achieved by depleting NA through the inhibition of cDVC hindbrain A2 neurons by 6-OHDA in the presence of systemic LPS-induced neuroinflammation (Fig. 2).

A qRT-PCR experiment was conducted to evaluate the mRNA expression of inflammatory markers in the PFC and hippocampus at the molecular level. Our observations indicated that the VPA animal model, which received VEH-saline icv. + LPS i.p. treatment, exhibited a significant increase in NF- $\kappa$ B gene expression at the PFC compared to the VPA-controlled groups (Fig. 3A). In addition, the administration of LPS



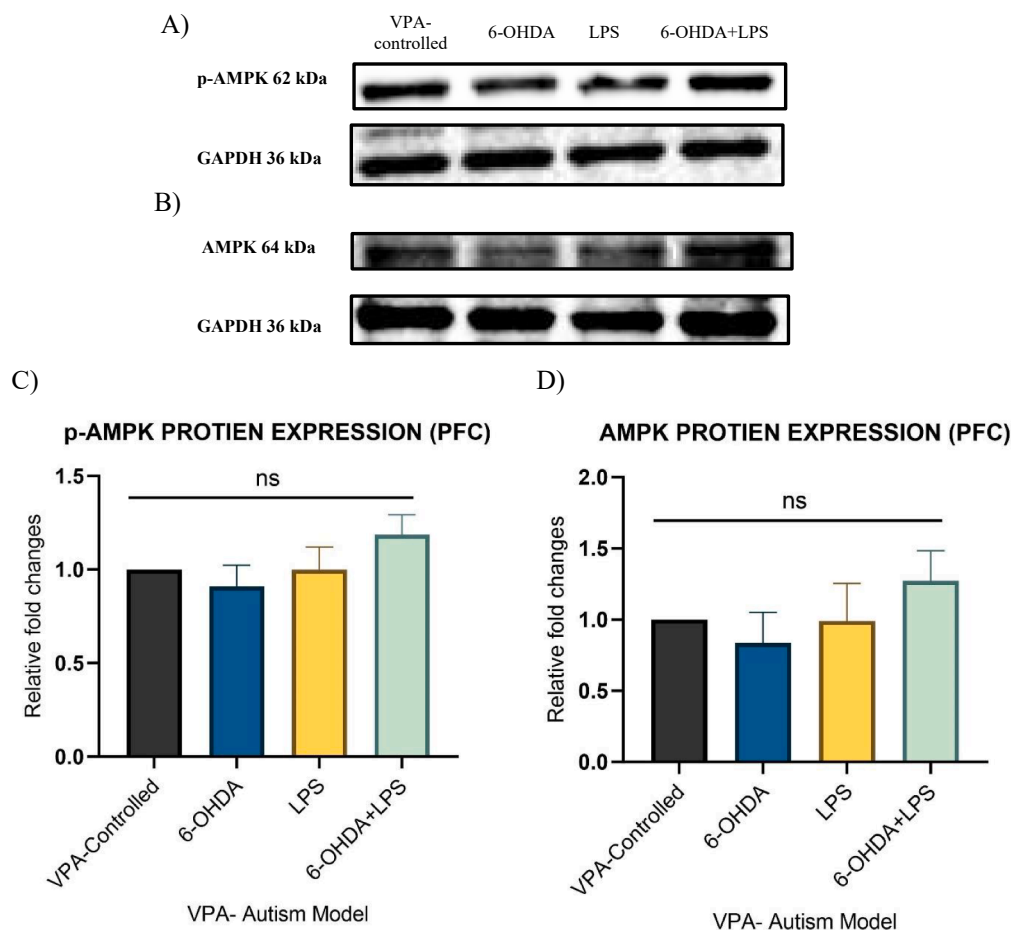


**Fig. 6.** The effect of 6-OHDA and LPS treatment on the p-AMPK and AMPK protein expression at PFC area in VPA-autism model. (A) p-AMPK and (B) AMPK Protein samples were analyzed using western blot technique. GAPDH was used as loading control. (C) represented relative changes in the level of p-AMPK protein compared to controlled group. (D) represented relative changes in the level of AMPK protein compared to controlled group. Data are shown as the mean  $\pm$  SEM ( $n = 3$ ) and no significant differences between treatment groups.

resulted in a considerable upregulation of the IL-6 gene expression in the PFC as compared to the VPA-controlled groups, as shown in Fig. 3B. Furthermore, the administration of LPS resulted in a substantial upregulation of the TNF- $\alpha$  gene expression in the hippocampus, as observed in comparison with the VPA-controlled groups (Fig. 4C). The data suggest that when LPS is administered systemically in the VPA autism model, it produces pro-inflammatory markers such as NF- $\kappa$ B and IL-6 in the PFC and TNF- $\alpha$  in the hippocampus. These findings align with a previous study conducted by Nadeem et al., 2020.

In addition, the mRNA levels of inflammatory markers, specifically NF- $\kappa$ B, IL-6, and TNF- $\alpha$ , in the PFC and hippocampus of the VPA autism model treated with 6-OHDA icv. + VEH-saline i.p. were quantified. Our data indicated a notable increase in the expression of mRNA inflammatory markers, such as NF- $\kappa$ B, IL-6, and TNF- $\alpha$ , in the PFC compared to the VPA-controlled group. This difference was statistically significant, as shown in Fig. 3A, B, and C. On the other hand, the markers exhibited a slightly higher level of expression in the hippocampal brain area compared to the autism-controlled group (Fig. 4A, B, and C). The data suggest that the direct injection of 6-OHDA icv. alone can cause the generation of pro-inflammatory cytokines in the PFC and hippocampus regions of the brain, potentially worsening the severity of ASD. In other words, the suppression of cDVC A2 NA neurons has been robust enough to induce the release of the inflammatory markers, IL-6 and TNF- $\alpha$ , specifically in the PFC. The obtained data aligns with prior research that observed an increase in inflammatory markers in the 6-OHDA produced

PD model (Ham et al., 2022; Tiwari et al., 2021; Li et al., 2008).

Moreover, the mRNA levels of inflammatory markers, such as NF- $\kappa$ B, IL-6, and TNF- $\alpha$ , in the PFC and hippocampus of the VPA autism model treated with 6-OHDA icv. and LPS i.p. were analyzed. Our data indicated that the activation of inflammatory markers, such as NF- $\kappa$ B, in the PFC brain region was considerably higher compared to the VPA-controlled group (Fig. 3A). In addition, the combination group exhibited a modest increase in the production of IL-6 and TNF- $\alpha$  markers at the PFC compared to the VPA-controlled group (Fig. 3B, C). Furthermore, the combination group exhibits a slight enhancement in the production of the NF- $\kappa$ B marker in the hippocampus, as compared to the VPA-controlled group (Fig. 4A). Our findings suggest that the administering of 6-OHDA icv. + LPS i.p. to rats treated with VPA can increase the production of pro-inflammatory markers in the PFC and hippocampal regions of the brain. This could potentially impact the severity of ASD. The observations presented here align with prior research that showed the ability of the 6-OHDA + LPS combination to produce inflammation in specific brain areas in the 6-OHDA PD model (Hritcu et al., 2011; Koprach et al., 2008; Pott Godoy et al., 2008).

However, our results indicate a significant decrease in the gene expression of IL-6 and TNF- $\alpha$  at the PFC in the combination group (6-OHDA + LPS) compared to the group treated with only 6-OHDA. Furthermore, there was a notable decrease in IL-6 gene expression in the hippocampus as compared to the LPS group. To mitigate these disparities, we can employ 6-OHDA + LPS in the VPA-autism model to

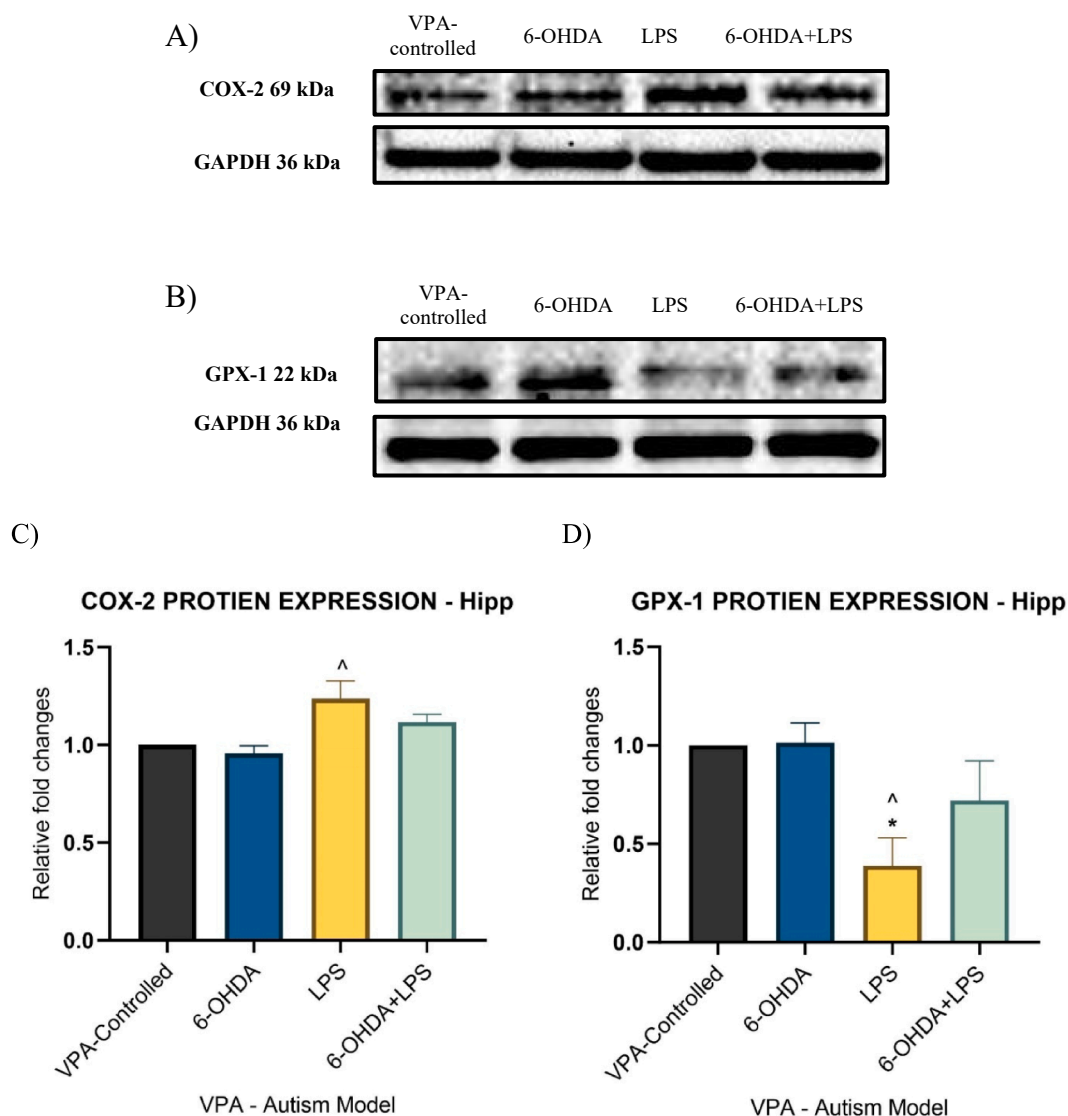


**Fig. 7.** The effect of 6-OHDA and LPS treatment on A) COX-2 and B) GPX-1 protein's expression at hippocampus area in VPA-autism model. (A) COX-2 Protein samples were analyzed using western blot technique. GAPDH was used as loading control. (C) represented relative changes in the level of COX-2 protein compared to controlled group. (B) GPX-1 Protein samples were analyzed using western blot technique. GAPDH was used as loading control. (C) represented relative changes in the level of GPX-1 protein compared to controlled group. Fig. 7A-C data are shown as the mean  $\pm$  SEM (n = 3) and considered statistically significant with  $P < 0.05$  (6-OHDA Vs LPS). Fig. 7B-D data are shown as the mean  $\pm$  SEM (n = 3) and considered statistically significant with  $*P < 0.05$  (VPA-controlled Vs LPS) and  $P < 0.05$  (6-OHDA Vs LPS).

investigate many parameters that may impact the neuroinflammation state in the autism model. These elements include compensatory mechanisms, the specific location of 6-OHDA injection, the dosage of either 6-OHDA or LPS and the method of LPS administration.

Changes in COX-2 levels have been documented in several neurological illnesses, potentially playing a role in the development of anomalies in the nervous system. There is evidence suggesting a correlation between the COX-2 encoding gene (Prostaglandin-Endoperoxide Synthase 2 - PTGS2 polymorphism) and ASD. The cortical COX-2 immunoreactivity in patients with Rett syndrome, a kind of ASD, has exhibited a reduction by 16 levels (Tamiji & Crawford, 2011, Yui et al., 2022). Our data revealed that the group of VPA rats treated with VEH-saline icv. + LPS i.p. was the only group that significantly increased COX-2 protein expression in the PFC region compared to the VPA-controlled and 6-OHDA treated groups (Fig. 5A), as well as in the hippocampus compared to the VPA-controlled group (Fig. 7A). The findings align with the prior research, which discovered that injecting LPS

enhances microglia activation and increase inflammatory markers (Kaizaki et al., 2013). The findings suggest that the induction of noradrenergic lesioning (specifically targeting A2 cells) using 6-OHDA did not result in an elevation of COX-2 expression in either of the regions studied within the VPA autism model. The observations presented here align with a prior study that observed no disparities in COX-2 expression between the LPS and combination group in the 6-OHDA model (Pott Godoy et al., 2008; O'Neill et al., 2021). We suggest that the unaltered COX-2 protein expressions seen in the 6-OHDA or combination groups resulted from compensatory mechanisms.

Moreover, the protein expression levels of the antioxidant marker GPx-1 in the PFC and hippocampal areas of the VPA autism model were evaluated (Fig. 5B and B). Our observations indicated that the VPA animals' model, which received administration of VEH-saline icv. together with i.p. injection of LPS, exhibited a more pronounced decrease in GPx-1 protein expression in the PFC and hippocampal regions compared to the VPA-controlled groups. Furthermore, the LPS

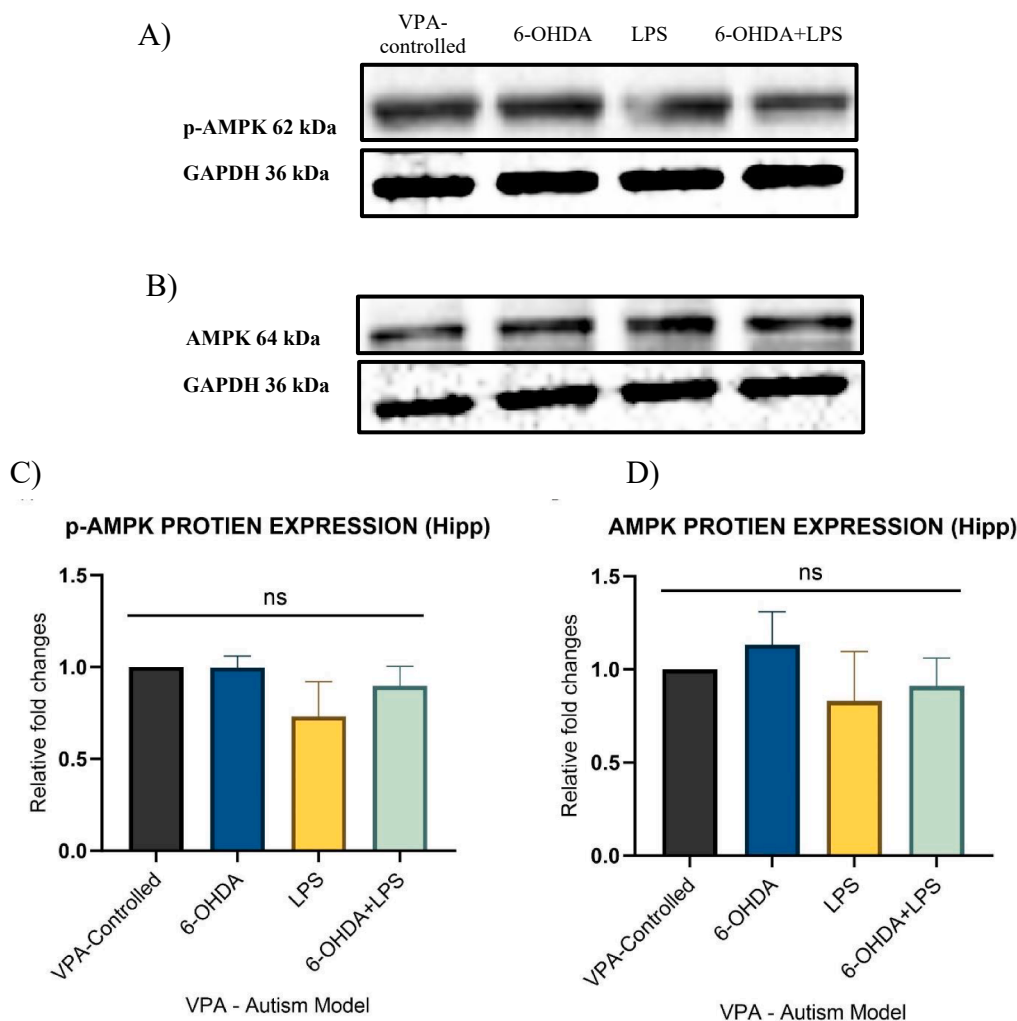


**Fig. 8.** The effect of 6-OHDA and LPS treatment on the p-AMPK and AMPK protein expression at hippocampus area in VPA-autism model. (A) p-AMPK and (B) AMPK Protein samples were analyzed using western blot technique. GAPDH was used as loading control. (C) represented relative changes in the level of p-AMPK protein compared to controlled group. (D) represented relative changes in the level of AMPK protein compared to controlled group. Data are shown as the mean  $\pm$  SEM (n = 3) and no significant differences between treatment groups.

group decreased in GPx-1 levels in the hippocampal region as compared to the 6-OHDA group. The findings suggest that the administration of LPS in the VPA autism model led to an elevation in oxidant activity via suppressing the expression of GPx-1 protein in the PFC and hippocampal areas (Fig. 5B, Fig. 7B). The findings of our study align with prior research that observed a decrease in GPx-1 levels in specific brain areas following LPS injection (Abdel-Salam et al., 2014).

Furthermore, the VPA autism model which treated with 6-OHDA icv. + LPS i.p., exhibited a notable reduction in the protein expression of GPx-1 in the PFC area, particularly when compared to the VPA-controlled group (Fig. 5B). The expression of the GPx-1 protein in the 6-OHDA group was marginally lower than that in the VPA-controlled group, specifically in the PFC area. The results suggest that the destruction of noradrenergic cells, specifically A2 cells, caused by 6-OHDA may contribute to a decrease in GPx-1 protein expression, particularly in the PFC area in the VPA autistic model. No significant disparity in protein expression of the GPx-1 antioxidant marker was detected between the LPS group and the combination group (6-OHDA + LPS) in both the PFC and hippocampal brain regions of the VPA autism model (Fig. 5B, Fig. 7B). These results confirm earlier findings that indicate a reduced level of GPx-1 activity in specific brain regions in the autism model (Nadeem et al., 2019). Additionally, other studies have

demonstrated that administering antioxidant compounds can lessen the neurotoxic effects of a PD model induced by 6-OHDA (Moshahid et al., 2010; Ridet et al., 2006).

The western blot approach was used to evaluate the protein expression levels of p-AMPK and AMPK in the PFC and hippocampal brain regions of the VPA autism model. This assessment is shown in Fig. 6 and Fig. 8. Our data indicated that there were no notable variations among the treatment groups in terms of p-AMPK and AMPK protein expression levels at the PFC and hippocampus in the VPA animal model. The data suggests that the cDVC p-AMPK pathway might not be implicated in the effect of provoking the PFC or hippocampal inflammatory mediators through A2 NA firing inhibition in the VPA-autistic model. This disruption is consistent with prior research, which discovered that the VPA autism model demonstrated an elevated level of p-AMPK at both the gene and protein levels (Servadio et al., 2018). Further research is required to determine the innervations of the hindbrain AMPK signaling pathways in various brain regions subjected to the neurodiversity caused by ASD.

The data acquired from this work revealed, for the first time, that the 6-OHDA icv. inhibited the cDVC A2 NA neurons elevate some important inflammatory markers in the PFC and to a lesser extent in the hippocampus in the VPA-autism model. Therefore, our data indicate that the

innervation of cDVC NA may play a significant role in safeguarding the developing process of the PFC and hippocampus by mitigating inflammation. Thus, A2 NA neurons have the potential to serve as a promising target for the future treatment and management of ASD.

## Funding

This research was funded by the Researchers Support Project number (RSPD2024R834), King Saud University, Riyadh, Saudi Arabia.

## Declaration of Competing Interest

The authors declare that they have no known competing financial interests or personal relationships that could have appeared to influence the work reported in this paper.

## Acknowledgments

The authors extend their appreciation to the Research Supporting Project number (RSPD2024R834), King Saud university, Riyadh, Saudi Arabia for funding this research work.

## References

- Abdel-Salam, O.M.E., Youness, E.R., Mohammed, N.A., Morsy, S. M.Y., Omara, E.A., Sleem, A.A., 2014. Citric Acid Effects on Brain and Liver Oxidative Stress in Lipopolysaccharide-Treated Mice. *Journal of Medicinal Food* 17 (5), 588–598. <https://doi.org/10.1089/jmf.2013.0065>.
- Alhamami, H.N., Uddin, M.M., Mahmood, A.S.M.H., Briski, K.P., 2018. Lateral but not medial hypothalamic AMPK activation occurs at the hypoglycemic nadir in insulin-injected male rats: impact of caudal dorsomedial hindbrain catecholamine signaling. *Neuroscience* 379 (March), 103–114. <https://doi.org/10.1016/j.neuroscience.2018.03.001>.
- Angoa-pérez, M., Kane, M.J., Briggs, D.I., Francescutti, D.M., Kuhn, D.M., 2013. Marble burying and nestlet shredding as tests of repetitive. Compulsive-like Behaviors in Mice. *Journal of Visualized Experiments*, 82. December, 1–7. doi:10.3791/50978.
- Banker, S.M., Gu, X., Schiller, D., Foss-Feig, J.H., 2021. Hippocampal contributions to social and cognitive deficits in autism spectrum disorder. *Trends Neurosci.* 44 (10), 793–807. <https://doi.org/10.1016/j.tins.2021.08.005>.
- Bjørklund, G., Tinkov, A.A., Hosnedlová, B., Kizek, R., Ajsuvakova, O.P., Chirumbolo, S., Skalnova, M.G., Peana, M., Dadar, M., El-Ansary, A., Qasem, H., Adams, J.B., Aaseth, J., Skalny, A.V., 2020. The role of glutathione redox imbalance in autism spectrum disorder: a review. *Free Radic. Biol. Med.* 160 (February), 149–162. <https://doi.org/10.1016/j.freeradbiomed.2020.07.017>.
- Bódi, V., Májer, T., Kelemen, V., Világi, I., Szűcs, A., Varró, P., 2022. Alterations of the hippocampal networks in valproic acid-induced rat autism model. *Front. Neural Circuits* 16 (February), 1–12. <https://doi.org/10.3389/fncir.2022.772792>.
- Donovan, A.P.A., Basson, M.A., 2017. The neuroanatomy of autism - a developmental perspective. *J. Anat.* 44 (August 2016), 4–15. <https://doi.org/10.1111/joa.12542>.
- Favre, M.R., Barkat, T.R., LaMendola, D., Khazen, G., Markram, H., Markram, K., 2013. General developmental health in the VPA-rat model of autism. *Front. Behav. Neurosci.* 7 (JUL), 1–11. <https://doi.org/10.3389/fnbeh.2013.00088>.
- Ham, H.J., Yeo, I.J., Jeon, S.H., Lim, J.H., Yoo, S.S., Son, D.J., Jang, S.S., Lee, H., Shin, S. J., Han, S.B., Yun, J.S., Hong, J.T., 2022. Botulinum toxin A ameliorates neuroinflammation in the MPTP and 6-OHDA-induced parkinson's disease models. *Biomol. Ther.* 30 (1), 90–97. <https://doi.org/10.4062/biomolther.2021.077>.
- Hirsch, M.M., Deckmann, I., Fontes-Dutra, M., Bauer-Negrini, G., Della-Flora Nunes, G., Nunes, W., Rabelo, B., Riesgo, R., Margis, R., Bambini-Junior, V., Gottfried, C., 2018. Behavioral alterations in autism model induced by valproic acid and translational analysis of circulating microRNA. *Food Chem. Toxicol.* 115 (March), 336–343. <https://doi.org/10.1016/j.fct.2018.02.061>.
- Hritcu, L., Ciobica, A., Stefan, M., Mihasan, M., Palamiuc, L., Nabeshima, T., 2011. Spatial memory deficits and oxidative stress damage following exposure to lipopolysaccharide in a rodent model of Parkinson's disease. *Neurosci. Res.* 71 (1), 35–43. <https://doi.org/10.1016/j.neures.2011.05.016>.
- Hyman, S.L., Levy, S.E., Myers, S.M., Kuo, D.Z., Apkon, S., Davidson, L.F., Bridgeman, C., 2020. Identification, evaluation, and management of children with autism spectrum disorder. *Pediatrics* 145 (1). <https://doi.org/10.1542/9781610024716-part01-ch002>.
- Kaizaki, A., Tien, L.-T., Pang, Y., Cai, Z., Tanaka, S., Numazawa, S., Bhatt, A.J., Fan, L.-W., 2013. Celecoxib reduces brain dopaminergic neuronal dysfunction, and improves sensorimotor behavioral performance in neonatal rats exposed to systemic lipopolysaccharide. *Journal of Neuroinflammation* 10 (1). <https://doi.org/10.1186/1742-2094-10-45>.
- Koprich, J.B., Reske-Nielsen, C., Mithal, P., Isacson, O., 2008. Neuroinflammation mediated by IL-1 $\beta$  increases susceptibility of dopamine neurons to degeneration in an animal model of Parkinson's disease. *Journal of Neuroinflammation* 5 (1). <https://doi.org/10.1186/1742-2094-5-8>.
- Li, L.Y., Zhao, X.L., Fei, X.F., Gu, Z.L., Qin, Z.H., Liang, Z.Q., 2008. Bilobalide inhibits 6-OHDA-induced activation of NF- $\kappa$ B and loss of dopaminergic neurons in rat substantia nigra. *Acta Pharmacol. Sin.* 29 (5), 539–547. <https://doi.org/10.1111/j.1745-7254.2008.00787.x>.
- Lord, C., Brugha, T.S., Charman, T., Cusack, J., Dumas, G., Frazier, T., Jones, E.J.H., Jones, R.M., Pickles, A., State, M.W., Taylor, J.L., Veenstra-VanderWeele, J., 2020. Autism spectrum disorder. *Nat. Rev. Dis. Primers* 6 (1). <https://doi.org/10.1038/s41572-019-0138-4>.
- Maenner, M.J., Warren, Z., Williams, A.R., Amoakohene, E., Bakian, A.V., Bilder, D.A., Shaw, K.A., 2023. Prevalence and characteristics of autism spectrum disorder among children aged 8 years—Autism and Developmental Disabilities Monitoring Network, 11 sites, United States, 2020. *MMWR Surveill. Summ.* 72 (2), 1. <https://doi.org/10.15585/mmwr.ss7202a1>.
- Moshahid, M., Ahmad, A., Ishrat, T., Khan, M.B., Hoda, N., Khuwaja, G., Shadab, S., Khan, A., 2010. Resveratrol attenuates 6-hydroxydopamine-induced oxidative damage and dopamine depletion in rat model of Parkinson's disease. *Brain Res.* 1328, 139–151. <https://doi.org/10.1016/j.brainres.2010.02.031>.
- Nadeem, A., Ahmad, S.F., Al-Harbi, N.O., Attia, S.M., Alshammari, M.A., Alzahrani, K.S., Bakheet, S.A., 2019. Increased oxidative stress in the cerebellum and peripheral immune cells leads to exaggerated autism-like repetitive behavior due to deficiency of antioxidant response in BTBR T + tf/J mice. *Prog. Neuropsychopharmacol. Biol. Psychiatry* 89 (September 2018), 245–253. <https://doi.org/10.1016/j.pnpbp.2018.09.012>.
- Nadeem, A., Ahmad, S. F., AL-Ayadhi, L. Y., Attia, S. M., Al-Harbi, N. O., Alzahrani, K. S., Bakheet, S. A. 2019. A Differential regulation of Nrf2 is linked to elevated inflammation and nitrate stress in monocytes of children with autism. *Psychoneuroendocrinology*, 113 (December 2019) 2020 104554. <https://doi.org/10.1016/j.psyneuen.2019.104554>.
- Nicolini, C., Fahnstock, M., 2018. The valproic acid-induced rodent model of autism. *Exp. Neurol.* 299, 217–227. <https://doi.org/10.1016/j.expneurol.2017.04.017>.
- Oliynyk, Z., Rudyk, M., Dovbynchuk, T., Dzubenko, N., Tolstanova, G., Skivka, L., 2023. Inflammatory hallmarks in 6-OHDA- and LPS-induced Parkinson's disease in rats. *Brain, Behavior, and Immunity - Health* 30 (March), 100616. <https://doi.org/10.1016/j.bbih.2023.100616>.
- O'Sullivan, J.B., Ryan, K.M., Curtin, N.M., Harkin, A., Connor, T.J., 2008. Noradrenergic reuptake inhibitors limit neuroinflammation in rat cortex following a systemic inflammatory challenge: implications for depression and neurodegeneration. *The International Journal of Neuropsychopharmacology* 12 (05), 687. <https://doi.org/10.1017/s146114570800967x>.
- Park, H.R., Lee, J.M., Moon, H.E., Lee, D.S., Kim, B.N., Kim, J., Kim, D.G., Paek, S.H., 2016. A short review on the current understanding of autism spectrum disorders. *Experimental Neurobiology* 25 (1), 1–13. <https://doi.org/10.5607/en.2016.25.1.1>.
- Pott Godoy, Tarelli, R., Ferrari, C.C., Sarchi, M.I., Pitossi, F.J., 2008. Central and systemic IL-1 exacerbates neurodegeneration and motor symptoms in a model of Parkinson's disease. *Brain* 131 (7), 1880–1894. <https://doi.org/10.1093/brain/awn101>.
- Rinaman, L., 2011. Hindbrain noradrenergic A2 neurons: Diverse roles in autonomic, endocrine, cognitive, and behavioral functions. *Am. J. Physiol. Regul. Integr. Comp. Physiol.* 300 (2), 222–235. <https://doi.org/10.1152/ajpregu.00556.2010>.
- Ruhela, R.K., Soni, S., Sarma, P., Prakash, A., Medhi, B., 2019. Negative geotaxis: An early age behavioral hallmark to VPA rat model of autism. *Ann. Neurosci.* 26 (1), 25–31. <https://doi.org/10.5214/ans.0972.7531.260106>.
- Ridet, J.-L., Bensaoud, J.-C., Déglon, N., Aebischer, P., Zurn, A.D., 2006. Lentivirus-mediated expression of glutathione peroxidase: Neuroprotection in murine models of Parkinson's disease. *Neurobiology of Disease* 21 (1), 29–34. <https://doi.org/10.1016/j.nbd.2005.06.003>.
- Scheggi, S., Guzzi, F., Braccagni, G., De Montis, Parenti, M., Gambarana, C., 2020. Targeting PPAR $\alpha$  in the rat valproic acid model of autism: focus on social motivational impairment and sex-related differences. *Molecular Autism* 11 (1). <https://doi.org/10.1186/s13229-020-00358-x>.
- Servadio, M., Manduca, A., Melancia, F., Leboffe, L., Schiavi, S., Campolongo, P., Palmery, M., Ascenzi, P., di Masi, A., Trezza, V., 2018. Impaired repair of DNA damage is associated with autistic-like traits in rats prenatally exposed to valproic acid. *Eur. Neuropsychopharmacol.* 28 (1), 85–96. <https://doi.org/10.1016/j.euroneuro.2017.11.014>.
- Tamiji, J., Crawford, D.A., 2011. The neurobiology of lipid metabolism in autism spectrum disorders. *Neurosignals* 18 (2), 98–112. <https://doi.org/10.1159/000323189>.
- Tiwari, P.C., Chaudhary, M.J., Pal, R., Kartik, S., Nath, R., 2021. Pharmacological, biochemical and immunological studies on protective effect of mangiferin in 6-hydroxydopamine (6-OHDA)-induced parkinson's disease in rats. *Ann. Neurosci.* 28 (3–4), 137–149. <https://doi.org/10.1177/09727531211051976>.
- Varghese, M., Keshav, N., Jacot-Descombes, S., Warda, T., Wicinski, B., Dickstein, D.L., Harony-Nicolas, H., De Rubeis, S., Drapeau, E., Buxbaum, J.D., Hof, P.R., 2017. Autism spectrum disorder: neuropathology and animal models. *Acta Neuropathol.* 134 (4), 537–566. <https://doi.org/10.1007/s00401-017-1736-4>.
- J.C.F. Vieira T.B. Bassani R.M. Santiago G. de O. Guaita J.M. Zanoveli C. da Cunha M.A. B.F. Vital Anxiety-like behavior induced by 6-OHDA animal model of Parkinson's disease may be related to a dysregulation of neurotransmitter systems in brain areas related to anxiety. *Behavioural Brain Research*, 371 May 2019 111981. <https://doi.org/10.1016/j.bbr.2019.111981>.
- Wang, Y., Zhou, Q., Zhang, X., Qian, Q., Xu, J., Ni, P., Qian, Y., 2017. Mild endoplasmic reticulum stress ameliorates lipopolysaccharide-induced neuroinflammation and cognitive impairment via regulation of microglial polarization. *Journal of Neuroinflammation* 14 (1). <https://doi.org/10.1186/s12974-017-1002-7>.
- Wei, H., Zou, H., Sheikh, A.M., Malik, M., Dobkin, C., Brown, W.T., et al., 2011. IL-6 is increased in the cerebellum of autistic brain and alters neural cell adhesion,

- migration and synaptic formation. *J. Neuroinflamm.* 8, 52. <https://doi.org/10.1186/1742-2094-8-52>.
- Wong, R.S.Y., 2022. Neuroinflammation in autism spectrum disorders: potential target for mesenchymal stem cell-based therapy. *Egyptian Journal of Neurology, Psychiatry and Neurosurgery* 58 (1). <https://doi.org/10.1186/s41983-022-00525-2>.
- Xie, J., Huang, L., Li, X., Li, H., Zhou, Y., Zhu, H., et al., 2017. Immunological cytokine profiling identifies TNF- $\alpha$  as a key molecule dysregulated in autistic children. *Oncotarget* 8, 82390–82398. <https://doi.org/10.18632/oncotarget.19326>.
- Yenkoyan, K., Grigoryan, A., Fereshteyan, K., Yepremyan, D., 2017. Advances in understanding the pathophysiology of autism spectrum disorders. *Behav. Brain Res.* 331 (May), 92–101. <https://doi.org/10.1016/j.bbr.2017.04.038>.
- Yui, K., Imataka, G., Yoshihara, S., 2022. Lipid-based molecules on signaling pathways in autism spectrum disorder. *Int. J. Mol. Sci.* 23 (17), 9803. <https://doi.org/10.3390/ijms23179803>.
- Zamberletti, E., Gabaglio, M., Woolley-Roberts, M., Bingham, S., Rubino, T., Parolaro, D., 2019. Cannabidiol Treatment ameliorates autism-like behaviors and restores hippocampal endocannabinoid system and glia alterations induced by prenatal valproic acid exposure in rats. *Front. Cell. Neurosci.* 13 (August), 1–15. <https://doi.org/10.3389/fncel.2019.00367>.
- Zeidan, J., Fombonne, E., Scoriah, J., Ibrahim, A., Durkin, M.S., Saxena, S., Yusuf, A., Shih, A., Elsabbagh, M., 2022. Global prevalence of autism: a systematic review update. *Autism Res.* 15 (5), 778–790. <https://doi.org/10.1002/aur.2696>.
- Zhao, J., Bi, W., Xiao, S., Lan, X., Cheng, X., Zhang, J., Lu, D., Wei, W., Wang, Y., Li, H., Fu, Y., Zhu, L., 2019. Neuroinflammation induced by lipopolysaccharide causes cognitive impairment in mice. *Sci. Rep.* 9 (1), 1–12. <https://doi.org/10.1038/s41598-019-42286-8>.
- Further reading**
- Gegotek, A., Skrzydlewska, E., 2022. Antioxidative and anti-inflammatory activity of ascorbic acid. *Antioxidants* 11 (10). <https://doi.org/10.3390/antiox11101993>.
- Hang, L., Wang, Z., Foo, A.S.C., Goh, G.W.Y., Choong, H.C., Thundiyil, J., Xu, S., Lam, K. P., Lim, K.L., 2021. Conditional disruption of AMP kinase in dopaminergic neurons promotes Parkinson's disease-associated phenotypes in vivo. *Neurobiol. Dis.* 161, 105560 <https://doi.org/10.1016/j.nbd.2021.105560>.
- Honarmand Tamizkar, K., Badrlou, E., Aslani, T., Brand, S., Arsang-Jang, S., Ghafouri-Fard, S., Taheri, M., 2021. Dysregulation of NF- $\kappa$ B-associated lncRNAs in autism spectrum disorder. *Front. Mol. Neurosci.* 14 <https://doi.org/10.3389/fnmol.2021.747785>.
- Ibrahim, B.A., Alenazi, F.S.H., Briski, K.P., 2015. Energy status determines hindbrain signal transduction pathway transcriptional reactivity to AMPK in the estradiol-treated ovariectomized female rat. *Neuroscience* 284, 888–899. <https://doi.org/10.1016/j.neuroscience.2014.10.068>.
- Kuo, H.Y., Liu, F.C., 2018. Molecular pathology and pharmacological treatment of autism spectrum disorder-like phenotypes using rodent models. *Front. Cell. Neurosci.* 12 (November) <https://doi.org/10.3389/fncel.2018.00422>.
- Malaguarnera, M., Khan, H., Cauli, O., 2020. Resveratrol in autism spectrum disorders: Behavioral and molecular effects. *Antioxidants* 9 (3), 1–13. <https://doi.org/10.3390/antiox9030188>.
- Miri, S., Rasooli, A., Brar, S.K., 2019. Data on changes of NF- $\kappa$ B gene expression in liver and lungs as a biomarker and hepatic injury in CLP-induced septic rats. *Data Brief* 25, 104117. <https://doi.org/10.1016/j.dib.2019.104117>.
- Peinnequin, A., Mouret, C., Birot, O., Alonso, A., Mathieu, J., Clarençon, D., Agay, D., Chancerelle, Y., Multon, E., 2004. Rat pro-inflammatory cytokine and cytokine related mRNA quantification by real-time polymerase chain reaction using SYBR green. *BMC Immunol.* 5, 1–10. <https://doi.org/10.1186/1471-2172-5-3>.
- Singh, R., Kisku, A., Kungumaraj, H., Nagaraj, V., Pal, A., Kumar, S., Sulakhiya, K., 2023. Autism spectrum disorders: a recent update on targeting inflammatory pathways with natural anti-inflammatory agents. *Biomedicines* 11 (1). <https://doi.org/10.3390/biomedicines11010115>.
- O'Neill, E., Griffin, É. W., O'Sullivan, R., Murray, C., Ryan, L., Yssel, J., Harkin, A., Cunningham, C. (2021). Acute neuroinflammation, sickness behavior and working memory responses to acute systemic LPS challenge following noradrenergic lesion in mice. *Brain, Behavior, and Immunity*, 94 July 2020 2021 357–368. <https://doi.org/10.1016/j.bbi.2020.12.002>.
- M. Saito M. Saito B.C. Das Involvement of AMP-activated protein kinase in neuroinflammation and neurodegeneration in the adult and developing brain. *International Journal of Developmental Neuroscience*, 77(December 2018) 2019 48 59. <https://doi.org/10.1016/j.ijdevneu.2019.01.007>.
- Ibrahim, B. A., Tamrakar, P., Gujar, A. D., Cherian, A. K., Briski, K. P., n.d., n.d. C aural Fourth Ventricular Administration of the AMPK Activator 5-Aminoimidazole- 4- Carboxamide-Riboside Regulates Glucose and Counterregulatory Hormone Profiles, Dorsal Vagal Complex Metabolosensory Neuron Function, and Hypothalamic Fos Expression. *Journal of Neuroscience Research* 91 ( 9 ), 1226 – 1238 <https://doi.org/10.1002/jnr.23230>.